Affine Perspective-Three-Point Problem —Supplementary Material—

Gaku Nakano
NEC Corporation, 1753 Shimonumabe, Kawasaki, Japan
g-nakano@nec.com

A. Complete algorithm of affine P3P solvers

The detailed algorithms of the proposed weak/para P3P solvers are shown in Algorithms 1 and 2, respectively. Three subroutines, the common pre-processing, a bi-quadratic solver for real solutions, and upgrading affine to perspective, are also shown in Algorithms 3 to 5, respectively. The symbol $\varnothing$ represents the empty set.

Algorithm 1: Weak P3P solver

Input : 3D points $\mathbf{X}_1, \mathbf{X}_2, \mathbf{X}_3$,
Normalized image points $\mathbf{m}_1, \mathbf{m}_2, \mathbf{m}_3$
Upgrade iterations $K \geq 0$
Output: Rotation $\mathtt{R}$, Translation $\mathbf{t}$

Compute $\mathbf{m}_g, \mathbf{X}_g, \mathbf{a}_{1,2}, \mathbf{v}_{1,2,3}$ ▷ Algorithm 3
$c_4 \leftarrow 1$
$c_2 \leftarrow \|\mathbf{v}_2\|^2 - \|\mathbf{v}_3\|^2$
$c_0 \leftarrow -(\mathbf{v}_2^\mathsf{T}\mathbf{v}_3)$
Solve $c_4\alpha^4 + c_2\alpha^2 + c_0 = 0$ ▷ Algorithm 4
$\beta \leftarrow \varnothing, \quad \mathtt{R} \leftarrow \varnothing, \quad \mathbf{t} \leftarrow \varnothing$
for each α
  if $\alpha = 0$ **and** $c_2 > 0$
    $\beta \leftarrow \beta \cup \{\pm\sqrt{c_2}\}$
  else
    $\beta \leftarrow \beta \cup \{c_0/\alpha\}$
if $\alpha \neq \varnothing$ **and** $\beta \neq \varnothing$
  for each α, β
    $\mathbf{r}_1 \leftarrow (\alpha\mathbf{v}_1 + \mathbf{v}_2)/\|\alpha\mathbf{v}_1 + \mathbf{v}_2\|$
    $\mathbf{r}_2 \leftarrow (\beta\mathbf{v}_1 + \mathbf{v}_3)/\|\beta\mathbf{v}_1 + \mathbf{v}_3\|$
    $\mathbf{r}_3 \leftarrow \mathbf{r}_1 \times \mathbf{r}_2$
    $z_0 \leftarrow (\mathbf{r}_1^\mathsf{T}\mathbf{a}_1 + \mathbf{r}_2^\mathsf{T}\mathbf{a}_2)/2$
    $\mathtt{R} \leftarrow \mathtt{R} \cup \{\,[\mathbf{r}_1, \mathbf{r}_2, \mathbf{r}_3]^\mathsf{T}\,\}$
    $\mathbf{t} \leftarrow \mathbf{t} \cup \{\,z_0\,[\mathbf{m}_g^\mathsf{T}, 1]^\mathsf{T} - \mathtt{R}\mathbf{X}_g\,\}$
  if $K > 0$
    Upgrade all $\mathtt{R}, \mathbf{t}$ ▷ Algorithm 5
return $\mathtt{R}, \mathbf{t}$

Algorithm 2: Para P3P solver

Input : 3D points $\mathbf{X}_1, \mathbf{X}_2, \mathbf{X}_3$,
Normalized image points $\mathbf{m}_1, \mathbf{m}_2, \mathbf{m}_3$
Upgrade iterations $K \geq 0$
Output: Rotation $\mathtt{R}$, Translation $\mathbf{t}$

Compute $\mathbf{m}_g, \mathbf{X}_g, \mathbf{a}_{1,2}, \mathbf{v}_{1,2,3}$ ▷ Algorithm 3
$(x_0, y_0) \leftarrow \mathbf{m}_g$
$k_1 \leftarrow -x_0 y_0$
$k_2 \leftarrow x_0^2 + 1$
$k_3 \leftarrow \mathbf{v}_2^\mathsf{T}\mathbf{v}_3(x_0^2+1) - \|\mathbf{v}_2\|^2 x_0 y_0$
$k_4 \leftarrow y_0^2 + 1$
$k_5 \leftarrow -(x_0^2+1)$
$k_6 \leftarrow \|\mathbf{v}_2\|^2 (y_0^2+1) - \|\mathbf{v}_3\|^2 (x_0^2+1)$
$c_4 \leftarrow k_1^2 k_5 + k_2^2 k_4$
$c_2 \leftarrow 2k_1 k_3 k_5 + k_2^2 k_6$
$c_0 \leftarrow k_3^2 k_5$
Solve $c_4\alpha^4 + c_2\alpha^2 + c_0 = 0$ ▷ Algorithm 4
$\beta \leftarrow \varnothing, \quad \mathtt{R} \leftarrow \varnothing, \quad \mathbf{t} \leftarrow \varnothing$
for each α
  if $\alpha = 0$ **and** $k_6/k_5 < 0$
    $\beta \leftarrow \beta \cup \{\pm\sqrt{-k_6/k_5}\}$
  else
    $\beta \leftarrow \beta \cup \{-(k_1\alpha^2 + k_3)/(k_2\alpha)\}$
if $\alpha \neq \varnothing$ **and** $\beta \neq \varnothing$
  for each α, β
    $\mathbf{p} \leftarrow \alpha\mathbf{v}_1 + \mathbf{v}_2$
    $\mathbf{q} \leftarrow \beta\mathbf{v}_1 + \mathbf{v}_3$
    $z_0 \leftarrow \frac{1}{2}\left(\sqrt{1+x_0^2}/\|\mathbf{p}\| + \sqrt{1+y_0^2}/\|\mathbf{q}\|\right)$
    $\mathbf{r}_3 \leftarrow$
     $z_0^2\left(\mathtt{I} - y_0 z_0 [\mathbf{p}]_\times + x_0 z_0 [\mathbf{q}]_\times\right)^{-1}(\mathbf{p} \times \mathbf{q})$
    $\mathbf{r}_1 \leftarrow z_0\mathbf{p} + x_0\mathbf{r}_3$
    $\mathbf{r}_2 \leftarrow z_0\mathbf{q} + y_0\mathbf{r}_3$
    $\mathtt{R} \leftarrow \mathtt{R} \cup \{\,[\mathbf{r}_1, \mathbf{r}_2, \mathbf{r}_3]^\mathsf{T}\,\}$
    $\mathbf{t} \leftarrow \mathbf{t} \cup \{\,z_0\,[\mathbf{m}_g^\mathsf{T}, 1]^\mathsf{T} - \mathtt{R}\mathbf{X}_g\,\}$
  if $K > 0$
    Upgrade all $\mathtt{R}, \mathbf{t}$ ▷ Algorithm 5
return $\mathtt{R}, \mathbf{t}$

Algorithm 3: Pre-processing

Input : 3D points $\mathbf{X}_1, \mathbf{X}_2, \mathbf{X}_3$,
Normalized image points $\mathbf{m}_1, \mathbf{m}_2, \mathbf{m}_3$
Output: 2D centroid $\mathbf{m}_g$, 3D centroid $\mathbf{X}_g$
Vectors $\mathbf{a}_1, \mathbf{a}_2$, Nullvectors $\mathbf{v}_1, \mathbf{v}_2, \mathbf{v}_3$

$\mathbf{X}_g \leftarrow \frac{1}{3}\sum_{i=1}^{3}\mathbf{X}_i$
$\mathbf{m}_g \leftarrow \frac{1}{3}\sum_{i=1}^{3}\mathbf{m}_i$
$\hat{\mathbf{X}}_1 \leftarrow \mathbf{X}_1 - \mathbf{X}_g, \quad \hat{\mathbf{X}}_2 \leftarrow \mathbf{X}_2 - \mathbf{X}_g$
$\hat{\mathbf{m}}_1 \leftarrow \mathbf{m}_1 - \mathbf{m}_g, \quad \hat{\mathbf{m}}_2 \leftarrow \mathbf{m}_2 - \mathbf{m}_g$
$[\mathbf{a}_1, \mathbf{a}_2] \leftarrow \left[\hat{\mathbf{X}}_1, \hat{\mathbf{X}}_2\right][\hat{\mathbf{m}}_1, \hat{\mathbf{m}}_2]^{-1}$
$\mathbf{n}_1 \leftarrow \begin{bmatrix} a_{21}a_{32} - a_{31}a_{22} \\ a_{31}a_{12} - a_{11}a_{32} \\ a_{11}a_{22} - a_{21}a_{12} \\ 0 \end{bmatrix}$
$\mathbf{n}_1 \leftarrow \mathbf{n}_1 / \|\mathbf{n}_1\|$
$\mathbf{n}_2 \leftarrow \begin{bmatrix} a_{22} \\ -a_{12} \\ 0 \\ a_{11}a_{22} - a_{12}a_{21} \end{bmatrix}$
$\mathbf{n}_2 \leftarrow \mathbf{n}_2 - (\mathbf{n}_1^\mathsf{T}\mathbf{n}_2)\mathbf{n}_1$
$\mathbf{n}_2 \leftarrow \mathbf{n}_2 / n_{24}$
$\mathbf{n}_3 \leftarrow \begin{bmatrix} -a_{21} \\ a_{11} \\ 0 \\ a_{11}a_{22} - a_{12}a_{21} \end{bmatrix}$
$\mathbf{n}_3 \leftarrow \mathbf{n}_3 - (\mathbf{n}_1^\mathsf{T}\mathbf{n}_3)\mathbf{n}_1$
$\mathbf{n}_3 \leftarrow \mathbf{n}_3 / n_{34}$
for each $\mathbf{n}_i, i \in \{1, 2, 3\}$
  $\mathbf{v}_i \leftarrow [n_{1i}, n_{2i}, n_{3i}]^\mathsf{T}$
return $\mathbf{m}_g, \mathbf{X}_g, \mathbf{a}_1, \mathbf{a}_2, \mathbf{v}_1, \mathbf{v}_2, \mathbf{v}_3$

Algorithm 4: Solve $c_4\alpha^4 + c_2\alpha^2 + c_0 = 0$

Input : Coefficients c_4, c_2, c_0
Output: Real-valued solution(s) α

for each $i \in \{0, 2, 4\}$
  $c_i \leftarrow c_i / \max(|c_4|, |c_2|, |c_0|)$
if $|c_4| \approx 0$ **and** $|c_2| \neq 0$ **and** $|c_0| \neq 0$
  $\alpha^2 \leftarrow -c_0/c_2$ ▷ $c_2\alpha^2 + c_0 = 0$
else if $|c_4| \neq 0$ **and** $|c_2| \neq 0$ **and** $|c_0| \approx 0$
  $\alpha^2 \leftarrow \{0,\ -c_2/c_4\}$ ▷ $c_4\alpha^4 + c_2\alpha^2 = 0$
else if $|c_4| \neq 0$ **and** $|c_2| \approx 0$ **and** $|c_0| \approx 0$
  $\alpha^2 \leftarrow 0$ ▷ $c_4\alpha^4 = 0$
else
  $D \leftarrow c_2^2 - 4c_0c_4$ ▷ Discriminant
  if $D < 0$
    $\alpha^2 \leftarrow \varnothing$
  else
    $q \leftarrow -(c_2 + \text{sign}(c_2)\sqrt{D})/2$
    $\alpha^2 \leftarrow \{q/c_4,\ c_0/q\}$
$\alpha \leftarrow \varnothing$
for each α^2
  if $\alpha^2 = 0$
    $\alpha \leftarrow \alpha \cup \{0\}$
  else if $\alpha^2 > 0$
    $\alpha \leftarrow \alpha \cup \{\pm\sqrt{\alpha^2}\}$
return α

Algorithm 5: Affine to perspective upgrade

Input : 3D points $\mathbf{X}_1, \mathbf{X}_2, \mathbf{X}_3$,
Normalized image points $\mathbf{m}_1, \mathbf{m}_2, \mathbf{m}_3$
Rotation $\mathtt{R}$,
Iterations $K > 0$, Tolerance $\epsilon_{\text{tol}} = 1e^{-5}$
Output: Rotation $\mathtt{R}$, Translation $\mathbf{t}$

for each $\{i, j\} \in \{\{1, 2\}, \{2, 3\}, \{3, 1\}\}$
  $\mathbf{c}_{ij} \leftarrow [\mathbf{m}_i^\mathsf{T}, 1]^\mathsf{T} \times [\mathbf{m}_j^\mathsf{T}, 1]^\mathsf{T}$
  $\mathbf{d}_{ij} \leftarrow \mathbf{X}_i - \mathbf{X}_j$
$k \leftarrow 0, \quad \theta \leftarrow \infty$
while $k \leq K$ **or** $\theta > \epsilon_{\text{tol}}$
  $k \leftarrow k + 1$
  $\Delta\mathbf{r} \leftarrow \begin{bmatrix} (\mathbf{c}_{12} \times \mathtt{R}\mathbf{d}_{12})^\mathsf{T} \\ (\mathbf{c}_{23} \times \mathtt{R}\mathbf{d}_{23})^\mathsf{T} \\ (\mathbf{c}_{31} \times \mathtt{R}\mathbf{d}_{31})^\mathsf{T} \end{bmatrix}^{-1} \begin{bmatrix} \mathbf{c}_{12}^\mathsf{T}\,\mathtt{R}\mathbf{d}_{12} \\ \mathbf{c}_{23}^\mathsf{T}\,\mathtt{R}\mathbf{d}_{23} \\ \mathbf{c}_{31}^\mathsf{T}\,\mathtt{R}\mathbf{d}_{31} \end{bmatrix}$
  $\theta \leftarrow \|\Delta\mathbf{r}\|$
  $\Delta\mathtt{R} \leftarrow \mathtt{I} + \sin\theta \left[\frac{\Delta\mathbf{r}}{\theta}\right]_\times + (1 - \cos\theta) \left[\frac{\Delta\mathbf{r}}{\theta}\right]_\times^2$
  $\mathtt{R} \leftarrow \Delta\mathtt{R}\,\mathtt{R}$
$\mathbf{t} \leftarrow -\begin{bmatrix} [\mathbf{m}_1]_\times \\ [\mathbf{m}_2]_\times \end{bmatrix}^+ \begin{bmatrix} [\mathbf{m}_1]_\times \mathtt{R}\mathbf{X}_1 \\ [\mathbf{m}_2]_\times \mathtt{R}\mathbf{X}_2 \end{bmatrix}$

B. Additional results on synthetic experiments

As described in Sec. 2.4, the accuracy of the affine approximations decreases as 2D points approach the image boundary, resulting in increasing errors. Figure B.1 shows a depth sensitivity test where image points are generated near the image border (withing the outer quarter of the width/height). The other settings were the same as in Sec. 4.1.1. Errors are slightly larger than in Fig. 2; however, we can observe similar tendencies. The proposed solvers converge almost within two iterations, highlighting the validity of the proposed update-scheme.

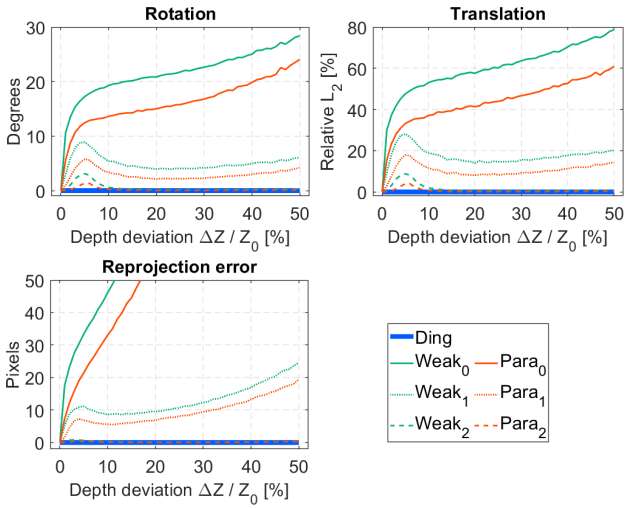

Figure B.1. Sensitivity against depth deviation with respect to image points close to the image border. Median values over 10^6 independent trials for each depth. Weak_2 and Para_2 almost overlap with Ding.

C. Additional results on real data experiments

C.1. Frequency of the real solutions

We evaluated the proportion of real-valued solutions returned by the proposed solvers and by the Ding solver across the two datasets. In this analysis, we counted the frequency with which each solver produced real solutions during the hypothesis-generation stage of RANSAC.

Tables C.1 and C.2 present the results for the EOPS and IMC2023 datasets, respectively. Across both datasets, our methods consistently produce two real solutions in nearly all instances. In contrast, the Ding solver exhibited a substantially wider distribution in the number of real solutions, typically yielding from 0 to 2 solutions, and occasionally even 3 or 4.

Table C.1. Percentage of the real solutions on the EPOS dataset. The dots · represent 0.00%.

Method	The number of real solutions				
	0	1	2	3	4
Ding	0.20	3.85	95.95	0.0001	0.0020
Weak_0	·	·	100.00	·	·
Weak_2	·	·	100.00	·	·
Para_0	·	·	100.00	·	·
Para_2	·	·	100.00	·	·

Table C.2. Percentage of the real solutions on the IMC2023 dataset. The dots · represent 0.00%.

Method	The number of real solutions				
	0	1	2	3	4
Ding	10.91	30.69	57.58	0.08	0.74
Weak_0	0.0002	·	99.9998	·	·
Weak_2	0.0003	·	99.9997	·	·
Para_0	·	·	100.00	·	·
Para_2	·	·	100.00	·	·

C.2. Performance w.r.t. runtime

We examined the runtime-dependent performance of each solver on the EPOS and IMC2023 datasets. Specifically, we varied the maximum number of RANSAC iterations from 10 to 3500 and computed the recall of the estimated poses relative to the ground truth as a function of the per-image processing time.

Figure C.1 presents the resulting recall–runtime curves, where the horizontal axis indicates the average processing time per image (in milliseconds) and the vertical axis reports the recall (in percent). Consistent with the synthetic evaluations, Weak_2 and Para_2 behave almost identically to the Ding solver, demonstrating comparable performance. On the other hand, Weak_0 and Para_0, which do not employ the refinement step, show performance saturation even when additional computation time is allowed.

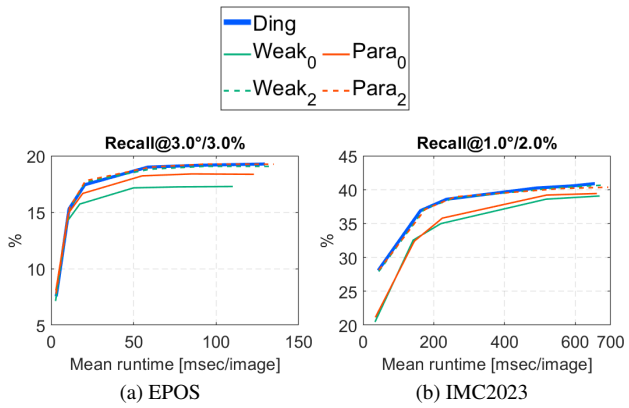

(a) EPOS (b) IMC2023

Figure C.1. Recall-runtime curve on the EPOS and IMC2023 datasets. Weak_2 and Para_2 almost overlap with Ding.

C.3. Quantitative evaluation per sequence

In this section, we present the experimental results for each sequence in the EPOS and IMC2023 datasets.

The EPOS dataset consists of three subsets: `T-LESS`, `YCB-V`, and `LM-O`, containing 3027, 2673, and 889 data instances, respectively. The experimental results of them are shown in Tabs. C.3 to C.5.

The IMC2023 dataset has four subsets: `Haiper`, `Heritage`, `Phototourism`, and `Urban`, containing 54, 247, 5461, and 271 data instances, respectively. The experimental results of them are shown in Tabs. C.6 to C.9.

Table C.3. Quantitative results on T-LESS of the EPOS dataset, which consists of 3027 instances. Recalls in percentages, and runtime and RANSAC iterations elapsed to process all data.

Method	Recall ($\epsilon_{\mathtt{R}}$ / $\epsilon_{\mathbf{t}}$) ↑							Time↓	Iters↓
	1°/1%	2°/2%	3°/3	5°/5%	7°/7%	10°/10%	20°/20%	(min.)	($\times 10^6$)
Ding +LO	1.0	7.5	17.9	32.7	41.7	48.5	56.1	10.60	1.58
Weak_2+LO	1.0	7.6	17.8	33.4	41.6	48.7	55.9	10.93	1.58
Para_2 +LO	0.9	7.6	17.8	33.4	41.7	48.7	56.0	10.99	1.58
Weak_0+LO	0.8	7.2	16.9	33.2	41.5	48.0	55.9	8.90	1.61
Para_0 +LO	0.9	7.3	17.6	33.4	42.0	48.8	56.7	10.02	1.58

Table C.4. Quantitative results on YCB-V of the EPOS dataset, which consists of 2673 instances. Recalls in percentages, and runtime and RANSAC iterations elapsed to process all data.

Method	Recall ($\epsilon_{\mathtt{R}}$ / $\epsilon_{\mathbf{t}}$) ↑							Time↓	Iters↓
	1°/1%	2°/2%	3°/3	5°/5%	7°/7%	10°/10%	20°/20%	(min.)	($\times 10^6$)
Ding +LO	1.3	11.3	25.3	47.7	60.9	71.4	80.5	3.19	0.58
Weak_2+LO	1.5	11.3	25.4	47.6	60.8	71.2	80.4	3.29	0.58
Para_2 +LO	1.4	11.4	25.4	47.4	60.7	71.1	80.4	3.31	0.58
Weak_0+LO	1.3	10.3	22.9	46.6	59.8	70.5	80.2	2.76	0.62
Para_0 +LO	1.3	10.5	24.8	47.4	60.4	70.7	80.3	3.03	0.59

Table C.5. Quantitative results on LM-O of the EPOS dataset, which consists of 889 instances. Recalls in percentages, and runtime and RANSAC iterations elapsed to process all data.

Method	Recall ($\epsilon_{\mathtt{R}}$ / $\epsilon_{\mathbf{t}}$) ↑							Time↓	Iters↓
	1°/1%	2°/2%	3°/3	5°/5%	7°/7%	10°/10%	20°/20%	(min.)	($\times 10^6$)
Ding +LO	0.1	1.0	2.7	12.3	27.4	45.0	71.3	0.32	0.16
Weak_2+LO	0.1	1.2	3.1	13.0	27.0	45.0	70.9	0.34	0.16
Para_2 +LO	0.1	1.2	2.7	12.9	27.6	44.8	70.9	0.35	0.16
Weak_0+LO	0.1	0.7	2.8	11.8	25.2	43.0	70.6	0.28	0.18
Para_0 +LO	0.2	0.9	3.1	12.6	26.6	44.0	71.7	0.31	0.16

Table C.6. Quantitative results on `Haiper` of the IMC2023 dataset, which consists of 54 instances. Recalls in percentages, and runtime and RANSAC iterations elapsed to process all data. Note the multiplication factor for the iterations is $\times 10^3$.

Method	Recall (ϵ_R / ϵ_t) ↑							Time↓	Iters↓
	0.1°/0.1%	0.1°/0.5%	0.5°/1.0%	1.0°/2.0%	2.0°/2.0%	3.0°/3.0%	5.0°/5.0%	(min.)	($\times 10^3$)
Ding +LO	3.7	80.2	100.0	100.0	100.0	100.0	100.0	0.01	2.1
Weak_2+LO	3.7	80.9	99.4	100.0	100.0	100.0	100.0	0.02	2.3
Para_2 +LO	3.7	79.0	100.0	100.0	100.0	100.0	100.0	0.02	2.1
Weak_0+LO	4.9	32.7	87.7	97.5	98.1	99.4	99.4	0.27	44.9
Para_0 +LO	4.9	52.5	95.1	100.0	100.0	100.0	100.0	0.15	23.5

Table C.7. Quantitative results on `Heritage` of the IMC2023 dataset, which consists of 247 instances. Recalls in percentages, and runtime and RANSAC iterations elapsed to process all data.

Method	Recall (ϵ_R / ϵ_t) ↑							Time↓	Iters↓
	0.1°/0.1%	0.1°/0.5%	0.5°/1.0%	1.0°/2.0%	2.0°/2.0%	3.0°/3.0%	5.0°/5.0%	(min.)	($\times 10^6$)
Ding +LO	45.3	58.6	74.9	79.5	80.0	80.7	81.9	1.29	0.16
Weak_2+LO	44.4	56.0	74.6	79.8	80.0	80.8	81.9	1.34	0.16
Para_2 +LO	44.4	57.1	75.0	79.6	80.2	81.0	81.9	1.33	0.16
Weak_0+LO	46.5	53.2	73.1	76.2	77.0	78.4	79.5	1.36	0.15
Para_0 +LO	44.0	51.8	68.5	72.9	74.6	76.3	77.2	1.58	0.17

Table C.8. Quantitative results on `Phototourism` of the IMC2023 dataset, which consists of 5461 instances. Recalls in percentages, and runtime and RANSAC iterations elapsed to process all data.

Method	Recall (ϵ_R / ϵ_t) ↑							Time↓	Iters↓
	0.1°/0.1%	0.1°/0.5%	0.5°/1.0%	1.0°/2.0%	2.0°/2.0%	3.0°/3.0%	5.0°/5.0%	(min.)	($\times 10^6$)
Ding +LO	2.7	11.5	21.9	38.4	39.0	50.0	62.6	35.32	1.31
Weak_2+LO	2.8	11.3	21.9	38.5	39.0	50.0	62.5	36.34	1.32
Para_2 +LO	2.8	11.3	22.0	38.2	38.8	49.8	62.6	36.08	1.32
Weak_0+LO	1.9	9.1	20.7	37.6	38.3	49.1	60.9	40.90	1.77
Para_0 +LO	2.0	9.3	20.7	37.7	38.3	49.1	61.0	40.35	1.68

Table C.9. Quantitative results on `Urban` of the IMC2023 dataset, which consists of 27 instances. Recalls in percentages, and runtime and RANSAC iterations elapsed to process all data.

Method	Recall (ϵ_R / ϵ_t) ↑							Time↓	Iters↓
	0.1°/0.1%	0.1°/0.5%	0.5°/1.0%	1.0°/2.0%	2.0°/2.0%	3.0°/3.0%	5.0°/5.0%	(min.)	($\times 10^3$)
Ding +LO	4.5	14.2	25.1	40.9	41.4	51.9	63.8	1.42	35.5
Weak_2+LO	4.6	13.8	25.0	40.9	41.5	51.9	63.8	1.53	35.7
Para_2 +LO	4.6	13.9	25.1	40.7	41.2	51.7	63.8	1.43	35.7
Weak_0+LO	3.6	11.1	23.5	39.8	40.5	50.7	62.0	2.08	39.1
Para_0 +LO	3.8	11.5	23.4	39.8	40.5	50.7	62.0	2.22	41.6